Effect of large-scale intermittency and mean shear on scaling-range exponents in a turbulent jet

J. Mi
Department of Mechanical Engineering, University of Adelaide, SA 5005, Australia

R. A. Antonia
Department of Mechanical Engineering, University of Newcastle, NSW 2308, Australia

(Received 21 November 2000; published 17 July 2001)

The present study investigates the combined impact of the intermittency associated with the turbulent-nonturbulent interface and the mean shear rate in an axisymmetric jet on the structure of turbulence in the scaling range, where the spectrum exhibits a power-law behavior. Second-order structure functions, autocorrelations of the dissipation rate, and spectra of both the longitudinal velocity fluctuation and the passive temperature fluctuation are measured at a distance of 40 diameter downstream from the nozzle exit. All the scaling range exponents are influenced by the large-scale intermittency and the mean shear. The scalar fluctuation is much more sensitive to the variation in large-scale intermittency than the velocity fluctuation.

DOI: 10.1103/PhysRevE.64.026302 PACS number(s): 47.27.−i

I. INTRODUCTION

The Kolmogorov 1941 [1] (or K41) similarity theory, which assumes local isotropy (or isotropy of the small-scale turbulence) and large Reynolds numbers, led to the result

$$\langle (\Delta u_r)^n \rangle = C_n \langle \epsilon \rangle^{n/3} r^{n/3} \tag{1}$$

when the separation r is within the inertial range (sometimes ''inertial subrange'') $\eta \ll r \ll L$. Here, $u(x)$ is the longitudinal velocity fluctuation, x is the longitudinal (axial) coordinate, $\Delta u_r \equiv u(x+r) - u(x)$ is the velocity increment, $\eta \equiv (\nu^3/\langle \epsilon \rangle)^{1/4}$ (angular brackets denote time averaging) is the Kolmogorov length scale, ϵ is the turbulent energy dissipation rate, L is the integral length scale of the turbulence, ν is the kinematic viscosity of the fluid, and C_n are constants which are likely to depend on the nature of the flow. There is now significant evidence to indicate that ''constant'' exponents, as implied by Eq. (1), are unlikely to apply at Reynolds numbers normally encountered in the laboratory [2] since a ''true'' inertial range in the sense of K41 is not observed. Exponent values quoted in the literature and, indeed, in the present paper, should be considered strictly as averages over what is generally referred to as the inertial range (IR) (the existence of such a range seems more justifiable when spectra are considered). (We shall continue to refer to the IR in this paper, although this only loosely refers to the range where the spectrum exhibits a power-law behavior). There is also enough evidence to indicate that, even in an asymptotic sense, the magnitudes of the exponents will differ from those given by Eq. (1), the departure being primarily attributed to the so-called ''internal'' small-scale intermittency arising from temporal and spatial fluctuations in ϵ. With the revised hypotheses of Kolmogorov [3] and Obukhov [4], relation (1) is replaced by

$$\langle \Delta u_r^n \rangle = C_n \langle \epsilon \rangle^{n/3} r^{\alpha_n}, \tag{2}$$

where the ''internal'' intermittency effect is reflected in the exponent α_n (here, the subscript r denotes integration over a linear dimension r). The autocorrelation of the dissipation rate ϵ exhibits a power-law behavior [5]

$$\langle \epsilon(x) \epsilon(x+r) \rangle \sim r^{-\mu}, \tag{3}$$

where r is in the IR. The exponent μ is a measure of the intermittency of $\epsilon(x)$, and is usually referred to as the intermittency exponent.

For the passive scalar case, relations analogous to Eqs. (1)–(3) have been obtained in the literature [5]. For simplicity, we shall write

$$\langle \Delta \theta_r^n \rangle \sim r^{n/3}, \tag{4}$$

$$\langle \Delta \theta_r^n \rangle \sim r^{\xi_n}, \tag{5}$$

and

$$\langle \epsilon_\theta(x) \epsilon_\theta(x+r) \rangle \sim r^{-\mu_\theta}. \tag{6}$$

Here, θ is the scalar fluctuation, ϵ_θ is the scalar dissipation rate, and μ_θ is the scalar intermittency exponent.

Much effort has been devoted to verifying the spectral relations which are equivalent to Eqs. (1) and (4) for $n=2$, viz.

$$\phi_u(k_1) = K_u \langle \epsilon \rangle^{2/3} k_1^{-5/3}, \tag{7}$$

$$\phi_\theta(k_1) = K_\theta \langle \epsilon \rangle^{-1/3} \langle \epsilon_\theta \rangle k_1^{-5/3}, \tag{8}$$

where K_u and K_θ are the ''spectral'' Kolmogorov and Obukhov–Corrsin constants. Confirmation of these relations, especially Eq. (7), has been claimed by many studies of turbulent flows at relatively high Reynolds numbers [6–11]. More recent studies [12–16] have indicated that the magnitudes of the exponents in Eqs. (7) and (8) increase gradually with the microscale Reynolds number R_λ [$\equiv u' \lambda/\nu$, where the longitudinal Taylor microscale $\lambda \equiv u'/(\partial u/\partial x)'$; herein the prime denotes the root-mean square, e.g., $u' \equiv \langle u^2 \rangle^{1/2}$]. It thus seems more reasonable to replace Eqs. (7) and (8) by

$$\phi_u(k_1) \sim k_1^{-m} \tag{9}$$

and

$$\phi_\theta(k_1) \sim k_1^{-m_\theta} \tag{10}$$

when k_1 is in the IR.

Strictly, Eqs. (1)–(10) apply to fully developed turbulence. However, it can be shown that the existence of large-scale intermittency, as measured by the factor γ (the fraction of time for which the flow is turbulent at a particular location), does not directly influence the exponents α_n, ξ_n, m, m_θ, μ, and μ_θ. A proof in the case of the scalar spectrum is as follows. When a turbulent/nonturbulent interface is present, we have

$$\langle \theta^2 \rangle = \gamma \langle \theta^2 \rangle_t + (1-\gamma) \langle \theta^2 \rangle_{\rm nt},$$

$$\langle \theta^2 \rangle = \int_0^\infty \phi_\theta(k_1) dk_1, \quad \langle \theta^2 \rangle_t = \int_0^\infty \phi_\theta^t(k_1) dk_1,$$

where the subscripts "t" and "nt" refer to fluctuations in the turbulent and nonturbulent regions, respectively. Since there should be no significant scalar (e.g., concentration, temperature) variation in the nonturbulent ambient flow, i.e., the temporal variation of $\theta_{\rm nt} = \Theta_a - \langle \Theta \rangle$ (where Θ_a is the instantaneous ambient scalar quantity) is negligible, $\phi_\theta(k_1)$ is closely approximated by $\gamma \phi_\theta^t(k_1)$. Given that $\phi_\theta^t(k_1) = g_t k_1^{-m_\theta^t}$ in the IR and $g_t = f(\langle \epsilon \rangle_t, \langle \epsilon_\theta \rangle_t, L)$, we have $\phi_\theta(k_1) = g k_1^{-m_\theta}$ with $g = \gamma f(\gamma \langle \epsilon \rangle_t, \gamma \langle \epsilon_\theta \rangle_t, L)$ and $m_\theta = m_\theta^t$. It follows that, while the "prefactor" g is a function of γ, the exponent m_θ does not depend on γ. Likewise, γ is also found to have no explicit influence on other scaling exponents (see Kuznetsov, Praskovsky, and Sabelnikov [17] for the effect of γ on μ).

To our knowledge, only one previous study [17] has investigated the effect of γ on the exponent μ (and the Kolmogorov constant C_2). By measuring μ and C_2 at different locations (and different values of γ) in five different shear flows, these authors found that both μ and C_2 vary with γ. However, it can be inferred from their data that R_λ has little influence on μ and C_2; their range of R_λ is 75–14 000 (see their Table I). They also reported that there was no effect on the spectral exponent m ($\approx 5/3$) from either γ or R_λ (this can be inferred from their Fig. 2). In contrast, Dowling and Dimotakis [18] and Mi [19] found that, in the far field of an axisymmetric jet at moderate Reynolds numbers of $R_d = 5000 - 40\,000$ (R_d is defined in Sec. II), the scaling exponent of the scalar spectrum m_θ increases significantly with the radial distance y. Since both γ and R_λ vary with y, one would not expect the magnitude of m_θ to be independent of these two parameters. However, it can be argued that the radial increase of m_θ cannot be attributed to the radial variation of R_λ. Sreenivasan [12,13] and Mydlarski and Warhaft [14] (also Antonia and Smalley [16]) observed that, in a fully turbulent ($\gamma = 1$) flow, the magnitude of m_θ increases with R_λ. The decrease in the magnitude of R_λ with increasing y (Fig. 1) should result in a reduction in the magnitude of m_θ as y increases. This is obviously contrary to the observations of Dowling and Dimotakis [18] and Mi [19]. It would thus appear that the radial variation of γ is the main cause for the radial increase in m_θ. However, the variation of γ should not be the only possible factor because, like γ, the mean velocity (shear) and temperature gradients vary with y. In the present study, we have measured structure functions, autocorrelations of dissipation rates, and frequency spectra of u and θ at various radial locations in the far field of an axisymmetric jet. The specific objective is to investigate how the IR exponents α_2, ξ_2, μ, μ_θ, m, and m_θ depend on γ and the mean shear rate. We surmise that both factors implicitly influence all the exponents (α_n, ξ_n, m, m_θ, μ, and μ_θ) but that the degree of influence may vary among exponents.

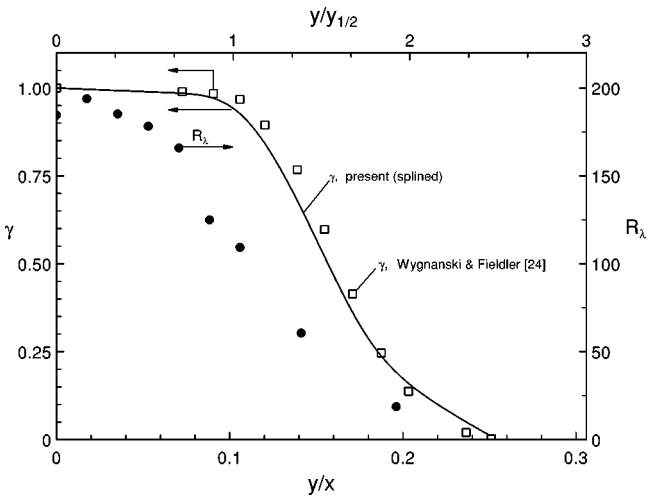

FIG. 1. Radial distributions of the intermittency factor γ (—) and microscale Reynolds number R_λ (●). The γ data (□) of Wygnanski and Fiedler [24] are included for comparison.

II. EXPERIMENTAL SETUP AND CONDITIONS

The jet facility consists of a vertical, cylindrical plenum chamber of 80 mm in diameter and 900 mm in length following an in-line diffuser and an electrical heater. (More details of the present experimental setup were provided in Mi, Nobes, and Nathan [20].) Filtered and compressed air was supplied through the heater and the plenum to a smooth contraction nozzle (exit diameter $d = 14$ mm). Heated and unheated air jets were used separately for temperature and velocity measurements. For the heated case, the facility and nozzle were insulated to achieve a uniform and symmetrical (about the nozzle axis) mean temperature profile at the exit, with the nominal value of $\Theta_0 = 50\,^\circ$C above ambient. The nominal exit Reynolds number $R_d \equiv U_0 d/\nu$ (where U_0 denotes the exit bulk velocity and ν is the kinematic viscosity) is about 16 000 for both cases. The present measurements were conducted at a distance of $x = 40d$ downstream from the nozzle exit. At this location, the center line mean velocity U_c was 2.7 m/s and the mean temperature Θ_c was 6.3 °C above ambient. On the axis, the rms values u_c' and θ_c' were approximately 0.68 m/s and 1.47 °C. Lateral distributions of $u'(y)$ and $\theta'(y)$ confirmed that the flow was approximately

TABLE I. Characteristic properties of the present jet at $x/d=40$.

U_c (m/s)	Θ_c (°C)	u_c' (m/s)	θ_c' (°C)	λ_c (mm)	η_c (mm)	$y_{1/2}$ (mm)	$y_{1/2}^{\Theta}$ (mm)
2.7	6.3	0.68	1.47	4.0	0.15	55	64

self preserving at $x/d=40$. The mean velocity half radius $y_{1/2}$ at which the local mean velocity is half the center line mean value is 55 mm. The mean temperature half radius is $=y_{1/2}^{\Theta}=64$ mm. Table I summarizes the characteristic properties of the jet at $x/d=40$.

The longitudinal velocity fluctuation u was obtained with a single hot-wire (5 μm tungsten; 1 mm long) probe with an overheat ratio of 1.8. The hot wire was operated with an in-house constant temperature anemometer. The hot wire was calibrated at the nozzle exit plane. The passive temperature fluctuation θ was measured with a cold wire (Wollaston Pt-10%Rh) of 0.63 μm in diameter, with an etched length of 0.8 mm. This cold wire was operated with a constant current (0.1 mA) circuit. The sensitivity of the wire to velocity fluctuations was negligible, and the wire length-to-diameter ratio (>1000) was sufficiently large to minimize any low-frequency attenuation of θ. The frequency response of the wire (the −3 dB frequency was estimated to be 4.5 kHz at 5 m/s) was also sufficient to avoid any high-frequency attenuation of θ. The u and θ signal outputs from the anemometer circuits were offset, amplified and then digitized on a PC using a 12-bit analog to digital converter. They were low-pass filtered at a cutoff frequency f_c chosen to eliminate high-frequency noise. The sampling frequency f_s was set to about $2f_c$. Record durations were in the range 40–50 s.

III. DATA PROCESSING AND METHOLODOGY

Velocity and temperature spatial increments were formed from the temporal increments $\Delta u_\tau=u(t)-u(t+\tau)$ and $\Delta\theta_\tau=\theta(t)-\theta(t+\tau)$, with the time delay $\tau=i/f_s$ (i is an integer $=1,2,3,\ldots$). This time delay was identified with the spatial increments Δu_r and $\Delta\theta_r$ by using Taylor's hypothesis in the form $r=-U\tau$, where U is the local mean velocity. This hypothesis was found to be reasonable on the axis of an axisymmetric jet by Mi and Antonia [21] who used two cold wires separated in the x direction and compared $\Delta\theta_r/r$ with $-\Delta\theta_\tau/(\tau U)$. Away from the axis, corrections to the hypothesis are needed for more accurate estimates of the mean dissipation rates [22].

In order to calculate the inertial-range exponents μ and μ_θ, the instantaneous energy and temperature dissipation rates, i.e., ϵ and ϵ_θ, were approximated by $\epsilon\sim(\partial u/\partial x)^2$ and $\epsilon_\theta\sim(\partial\theta/\partial x)^2$. These approximations, not exclusive for the present study, were used by most, if not all, of previous studies for μ and μ_θ. Also, Taylor's hypothesis, in the form $\partial/\partial x=-U^{-1}\partial/\partial t$, was used for these approximations. Estimates of μ and μ_θ were based on the following relations:

$$R_\epsilon=U^{-4}\left\langle\left[\frac{\partial u(x)}{\partial t}\right]^2\left[\frac{\partial u(x+r)}{\partial t}\right]^2\right\rangle\sim r^{-\mu}, \tag{11}$$

$$R_{\epsilon_\theta}=U^{-4}\left\langle\left[\frac{\partial\theta(x)}{\partial t}\right]^2\left[\frac{\partial\theta(x+r)}{\partial t}\right]^2\right\rangle\sim r^{-\mu_\theta}, \tag{12}$$

instead of Eqs. (3) and (6). In Eqs. (11) and (12), $r=-(i/f_s)U$ $[i=1,\ 2,\ 3,\ldots]$ and $\partial\sigma/\partial x\approx U^{-1}[\sigma(t+\Delta t)-\sigma(t)]/\Delta t$ (where $\sigma\equiv u$ or θ and the time interval $\Delta t=f_s^{-1}$). In the study of Champagne [10] on the fine-scale structure of jet turbulence, corrections due to the effect of a fluctuating convection velocity on Taylor's hypothesis $\partial/\partial x=-U^{-1}\partial/\partial t$ were applied. However, as shown analytically by Kuznetsov, Prakovsky, and Sabelnikov [17], the use of this does not affect μ (and, presumably, also μ_θ). Accordingly, no correction has been applied here.

The spectra ϕ_u and ϕ_θ were calculated directly from the signals $u(t)$ and $\theta(t)$ using the fast Fourier transform algorithm. Using Taylor's hypothesis, $k_1=2\pi fU^{-1}$ and Eqs. (9) and (10) can be replaced by

$$\phi_u(f)\sim f^{-m}, \tag{13}$$

$$\phi_\theta(f)\sim f^{-m_\theta}, \tag{14}$$

with $\int_0^\infty\phi_u(f)df=\langle u^2\rangle$ and $\int_0^\infty\phi_\theta(f)df=\langle\theta^2\rangle$.

IV. RESULTS AND DISCUSSION

The intermittency factor γ was estimated from the probability density function (pdf) of θ, using the method outlined in Bilger, Antonia, and Sreenivasan [23]. In this method, the pdf near the low temperature limit is assumed to represent the nearly Gaussian contribution from the ambient temperature fluctuations. The area under this nearly Gaussian distribution is equal to the probability of occurrence of ambient unheated fluid, i.e., $(1-\gamma)$. The resulting distribution of γ across the jet is shown in Fig. 1. For comparison, data obtained by Wygnanski and Fiedler [24], using different methods, also for a self-preserving axisymmetric jet (note that their data were reported against y/x) are included in Fig. 1. There is reasonable agreement between the two data sets. The magnitude of γ is almost unchanged over the central region, but decreases rapidly when $y/y_{1/2}>0.8$. Figure 1 also shows the radial variation of the microscale Reynolds number R_λ, which decreases from about 184 on the center line to 15 at $y/y_{1/2}=2$.

To investigate the effect of the mean shear, we measured the mean velocity U and mean dissipation rate $\langle\epsilon\rangle$ across the jet. Both local isotropy and Taylor's hypothesis were assumed in obtaining $\langle\epsilon\rangle$. Support for local isotropy in the far field of the jet, especially on the axis, was provided by Antonia and Mi [25] and Namazian, Schefer, and Kelly [26]. Radial profiles of the non-dimensional mean shear rate $S^*\equiv|\partial U/\partial y|(\nu/\langle\epsilon\rangle)^{1/2}$, along with U/U_c and $\langle\epsilon\rangle U_c^3 y_{1/2}$ are shown in Fig. 2. Clearly, S^* increases as y increases but varies slightly for $y<y_{1/2}$. Based on Figs. 1 and 2, it is evident that $\gamma\approx1$ for $y<y_{1/2}$, while for $y\geqslant y_{1/2}$, S^* is nearly unchanged. This important feature allows us to distinguish between the effects of γ and S^* unambiguously.

To check Eqs. (2) and (5) for $n=2$, $\langle\Delta u_r^2\rangle$ and $\langle\Delta\theta_r^2\rangle$ were calculated at various locations across the jet. Figure

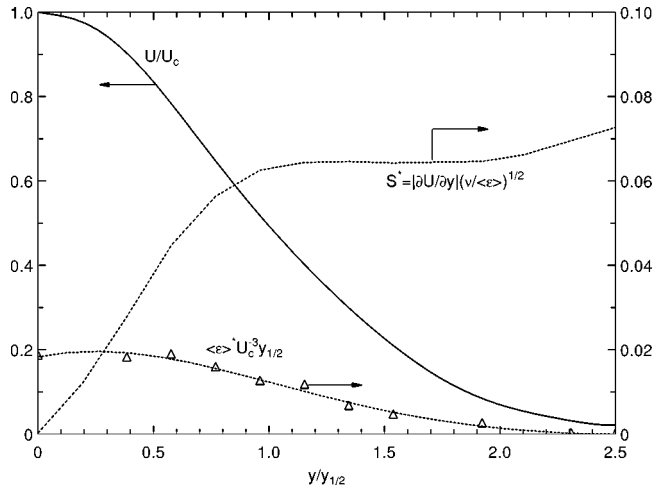

FIG. 2. Radial profiles of the nondimensional mean shear rate $S^* \equiv |\partial U/\partial y|(\nu/\langle\epsilon\rangle)^{1/2}$, U/U_c and $\langle\epsilon\rangle U_c^{-3} y_{1/2}$.

3(a) shows these structure functions, plotted against r, for different values of y. When log–log coordinates are used, these structure functions appear to exhibit a narrow power-law range at each y location, suggesting that both Eqs. (2) and (5) are approximately valid across the jet, regardless of γ and S^*. As noted earlier, there is strictly no power law; we ignore this here since the main interest is in the relative effects of γ and S^*. To estimate the scaling exponents α_2 and ξ_2, the optimum plateaus in the distributions of $r^{-\alpha_2^*}\langle \Delta u_r^2\rangle$ and $r^{-\xi_2^*}\langle \Delta \theta_r^2\rangle$ were identified by trying different values of α_2^* and ξ_2^*. Figure 3(b) presents the compensated data for the optimal values of α_2 ($\approx 2/3$) and ξ_2 (≈ 0.54–0.64) for $\gamma = 0.6$–1.0 and $S^* = 0 - 0.065$. Whereas α_2 does not appear to change across the flow, ξ_2 increases as y increases. This indicates that the r dependence of $\langle \Delta \theta_r^2\rangle$ is more sensitive to the variations of γ and S^* than that of $\langle \Delta u_r^2\rangle$. Further, α_2 is greater than ξ_2 for both $\gamma = 1$ ($S^* = 0$) and $\gamma < 1$ ($S^* > 0$). This result is consistent with that reported previously for $\gamma = 1$. For example, Antonia *et al.* [27] measured ξ_n on the axis of an axisymmetric jet ($x/d = 35$) for $n = 2 - 12$ and $R_\lambda = 850$. They compared ξ_n with α_n, as obtained by Anselmet *et al.* [28] in the same flow, and found that $\alpha_n > \xi_n$ for all n.

The autocorrelations R_ϵ and R_{ϵ_θ}, as defined by Eqs. (11) and (12), are plotted against $r/y_{1/2}$ in Fig. 4. A power-law behavior appears in both R_ϵ and R_{ϵ_θ} at each y location. The power-law exponents, indicated by straight lines, were obtained by plotting the compensated data of R_ϵ and R_{ϵ_θ}. On the axis ($\gamma = 1$ and $S^* = 0$), the magnitudes of μ and μ_θ (≈ 0.15 and 0.3) are smaller than those (0.25 and 0.38) recommended by Sreenivasan and Antonia [29] for fully developed turbulence. This difference may be in part due to the present small R_λ ($=184$). However, the use of different techniques for calculating the exponents is believed to be the main cause for the difference. Kuznetsov, Praskovsky, and Sabelnikov [17] used the same technique as for the present investigation and obtained a nearly identical value of μ at $\gamma = 1$ in three of their five shear flows with $R_\lambda = 140$–1700. Further, relative to the structure functions, the power-law region exhibited by the dissipation autocorrelations is more extended, starting from a smaller r. This tends to support the assumption of Monin and Yaglom [5] that Eq. (3) is valid down to scales of order of the Kolmogorov microscale.

Distributions of $\phi_u(f)$ and $\phi_\theta(f)$ are shown in Figs. 5(a) and 6(a) where the spectra are normalized by the corresponding rms values so that $\int \phi_u^*(f^*) df^* = \int \phi_\theta^*(f^*) df^* = 1$, where $f^* = f y_{1/2}/U_c$. To highlight the power-law region with less ambiguity than in Figs. 5(a) and 6(a), compensated distributions $f^{*m}\phi_u^*(f^*)$ and $f^{*m_\theta}\phi_\theta^*(f^*)$ are plotted against f^* in Figs. 5(b) and 6(b); the curves have been displaced for clarity. The power-law behaviors of ϕ_u and ϕ_θ are best identified by the plateaus in Figs. 5(b) and 6(b) (such plateaus cannot be found in plots of compensated structure

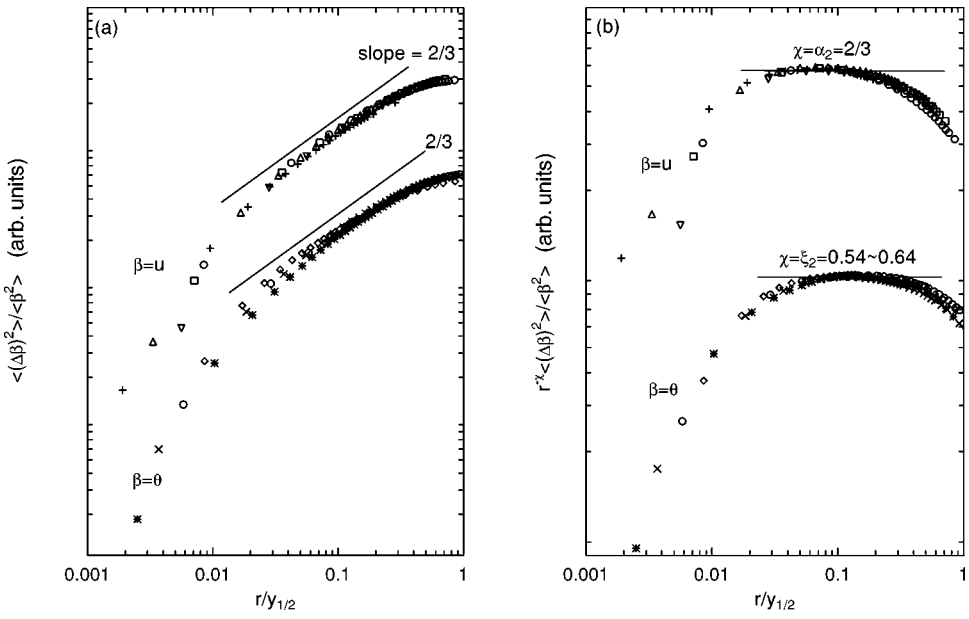

FIG. 3. Second-order structure functions of the longitudinal velocity fluctuation u and the scalar (temperature) fluctuation θ across the jet. Velocity ($\langle \Delta u_r^2\rangle/\langle u^2\rangle$): ($\bigcirc$), $y/y_{1/2} = 0.00$; ($\square$), 0.39; ($\triangledown$), 0.77; ($\triangle$), 1.15; and ($+$), 1.54. Temperature ($\langle \Delta \theta_r^2\rangle/\langle \theta^2\rangle$): ($\diamond$), 0.00; ($\bigcirc$), 0.71; ($\times$), 1.07; ($*$), 1.43.

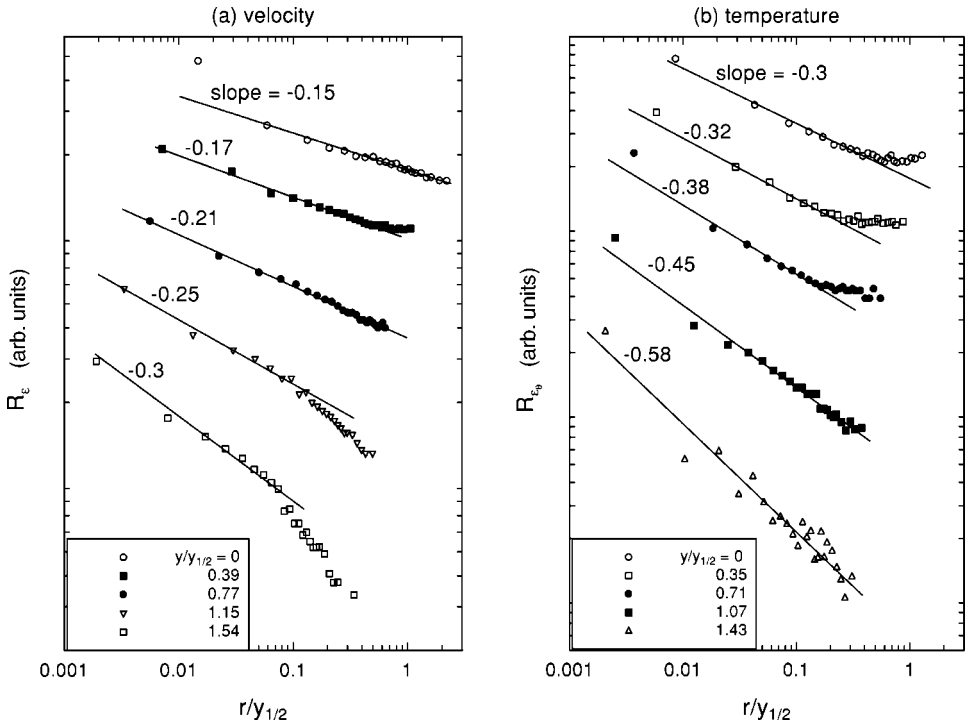

FIG. 4. Autocorrelations of the energy and temperature dissipation rates across the jet: (a) u; (b) θ.

functions). Also, both $m \approx 1.5$ and $m_\theta \approx 1.4$ deviate significantly from "5/3" on the jet axis ($\gamma = 1$ and $S^* = 0$). Consistently with the investigation of Dowling and Dimotakis [18] for $\phi_\theta(f)$, also in an axisymmetric jet flow, m and m_θ increase with y (and even exceed 5/3 near the edge of the jet). The increase of m and m_θ with y, as discussed below, is very likely due to the decrease in γ and the concomitant increase in S^*.

Figures 7(a) and 7(b) present μ and μ_θ as well as m and m_θ in terms of the normalized mean shear rate S^* for $y \leqslant y_{1/2}$. Over this region, $\gamma = 0.95 \sim 1$ so that the effect of γ should be negligible. As S^* increases from 0 to 0.065, all four exponents increase significantly. The mean shear rate thus has a strong influence on the scaling range exponents. We can also focus on only the "turbulent" region when $\gamma < 0.95$, by eliminating the nonturbulent parts of the velocity and temperature signals. A comparison between the spectrum of u and that of the conditional signal u_t, the "turbulent" portion of u, is shown in Fig. 8 for $y/y_{1/2} = 1.92$. Note that u_t was identified by selecting a threshold u_{TH} so that γ is given by the ratio of the sum of the periods (in the record) for which $u_t = u \geqslant u_{\mathrm{TH}}$ to the total record duration. Similar to the calculation of ϕ_u, the conditional spectrum ϕ_{u_t} was calculated directly from the signal u_t. A similar method was used

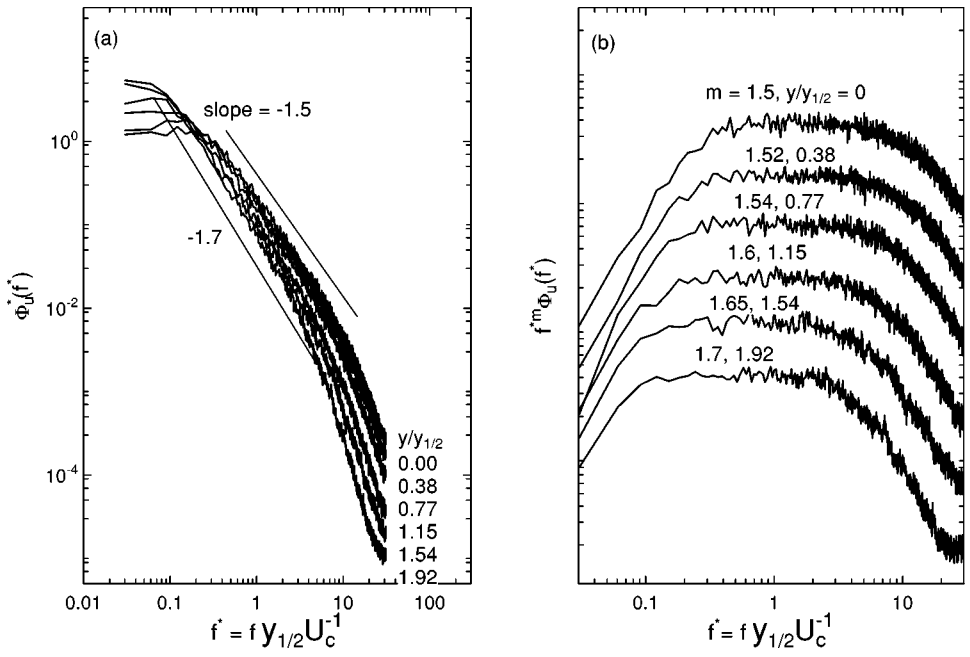

FIG. 5. Spectra of the longitudinal velocity fluctuation u across the jet: (a) $\phi_u^*(f)$; (b) $f^m \phi_u^*(f)$.

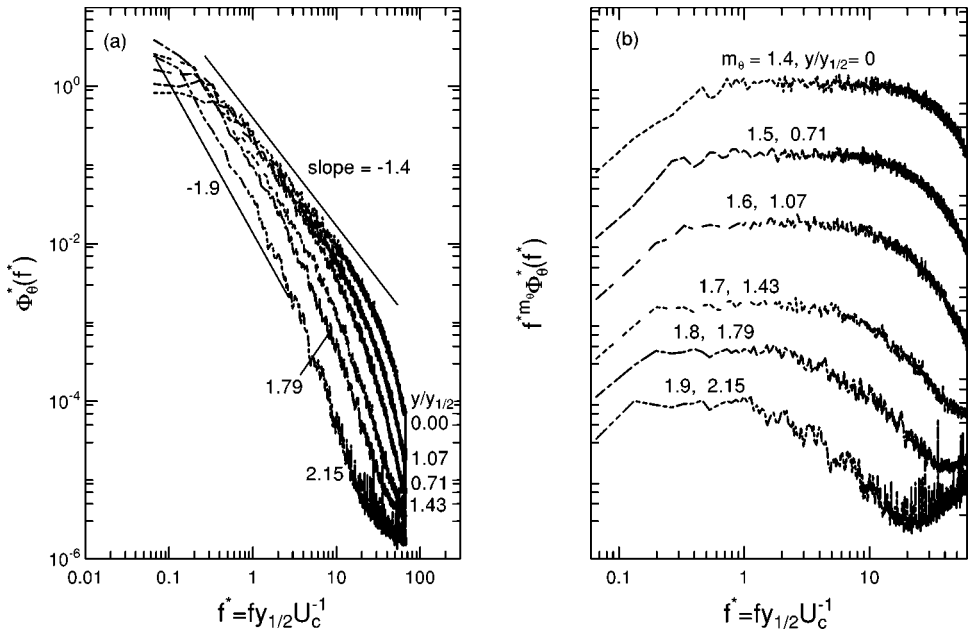

FIG. 6. Spectra of the scalar (temperature) fluctuation θ across the jet: (a) $\phi_\theta^*(f)$; (b) $f^{m_\theta}\phi_\theta^*(f)$.

for determining the conditional temperature spectra. As expected, the exponent m^t is significantly smaller than m_u; for $y/y_{1/2}=1.92$, m is about 1.7, whereas $m^t \approx 1.53$. This suggests that the large-scale intermittency has a strong influence on the IR exponents. We have also noticed that the exponents m^t and m_θ^t are greater than m and m_θ on the jet axis [as shown in Fig. 9(b)]. This discrepancy appears to be caused by the difference in S^* (0 on the axis and ~ 0.07 at $y/y_{1/2} > 1$).

It seems appropriate to now turn our attention to the effect of the large-scale intermittency. In Fig. 9(a), μ and μ_θ are plotted against γ. The μ data of Kuznetsov, Praskovsky, and Sabelnikov [17] for five different shear flows are included. Clearly, both exponents decrease as γ increases. This trend, observed in six different shear flows, should be quite general notwithstanding the dependence of μ, as observed by Kuznetsov, Praskovsky, and Sabelnikov [17], on the particular method used for its determination. Based on the data shown in Fig. 15 of their paper [and the present Fig. 9(a)], these investigators suggested that the γ dependence of μ on γ is universal. This, however, may not be the case, simply because the present value of μ is greater than their jet value by about 50% when $\gamma<1$. The main cause for the difference is not clear. Based on Fig. 7(a), it is surmised that the mean shear rate is an important contributor since S^* is quite large ($=0.065$–0.07) in the present jet when $\gamma<0.9$. It is unfortunate, however, that Kuznetsov, Praskovsky, and Sabelnikov did not consider the effect of the mean shear and did not

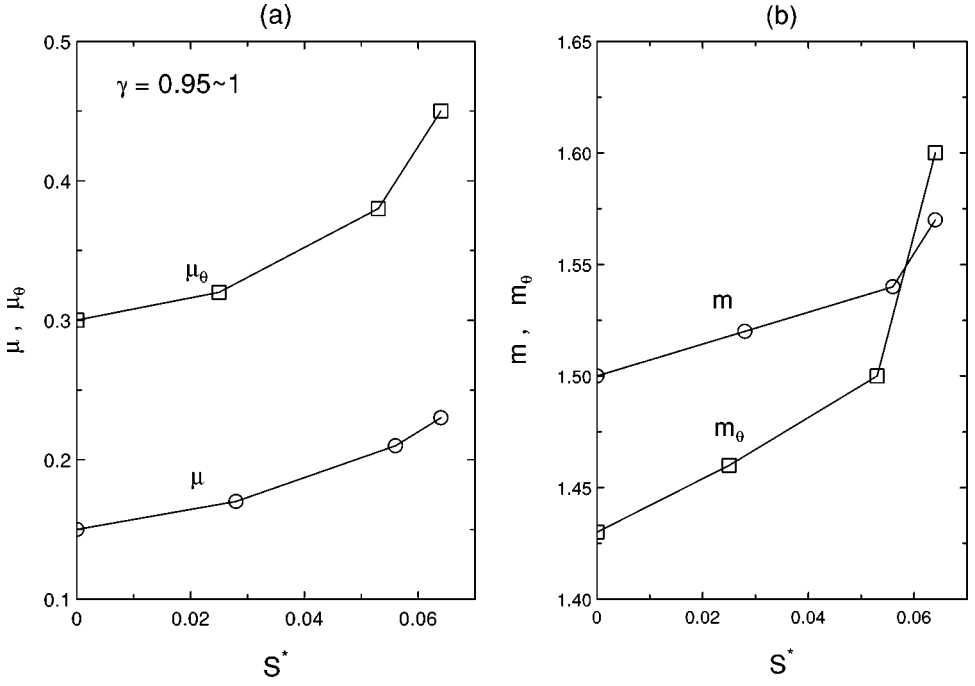

FIG. 7. Variation of the exponents μ, μ_θ, m, and m_θ with the mean shear rate S^* for $y \leqslant y_{1/2}$. (a) μ and μ_θ; (b) m and m_θ.

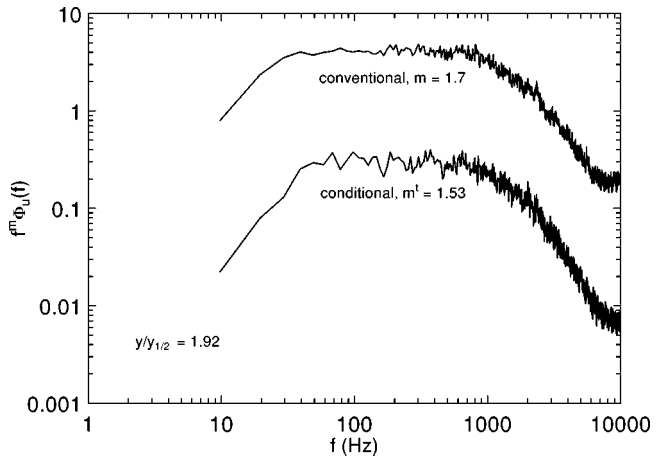

FIG. 8. Comparison between conventional and conditional spectra of u at $y/y_{1/2}=1.92$.

provide information to allow S^* to be estimated. Moreover, it is evident from Fig. 9(a) that μ_θ is greater than μ at any value of γ. This implies that the scalar dissipation rate is more intermittent than the energy dissipation rate, as noted by Sreenivasan and Antonia [29] in the context of $\gamma=1$.

Figure 9(b) shows that both m and m_θ decrease as γ increases; the trend is similar to that noted for μ and μ_θ. Also, m_θ has a greater dependence on y than m. Surprisingly, however, while α_2 remains close to 2/3 across the jet, m varies with γ and S^*. Equations (1) and (7) or (2) and (9) are simply related via a Fourier transform. When the power-law range has an infinite extent, m should be equal to $(1+\alpha_2)$. Similarly, $m_\theta \equiv 1+\xi_2$. The previous equalities do not hold when the Reynolds number is finite. Hou *et al.* [30] have emphasized that the finite power-law range makes the translation between Eq. (2) and Eq. (9) inexact, the error depending on the scaling exponent.

Apart from the effects of S^* and γ, the radial variation of the Reynolds number R_λ (Fig. 1) should also have an influence on the radial variations of m, m_θ, μ and μ_θ. Although we cannot separate the effect of R_λ from that due to γ and S^*, the radial decrease of R_λ (Fig. 1) should, as previously noted in Sec. I, result in a reduction in the magnitude of the exponents. Sreenivasan [12] reported that, in fully turbulent flows, m_θ and m_v (the exponent correspondent to the transverse velocity spectrum) increase with increasing R_λ and approach 5/3 at $R_\lambda \gtrsim 2000$. Sreenivasan and Dhruva [2] found, on the basis of $\langle (du)^6 \rangle$, that μ increases slightly with R_λ, approaching a value of about 0.32 at $R_\lambda \sim 104$; a similar trend was observed by Pearson [31]. These trends are clearly opposite to those observed here in Figs. 4–6, i.e., the exponents increase with y, whereas R_λ decreases with y (Fig. 1). It is therefore concluded that the observed radial increase of the exponents arises from the large-scale intermittency and mean shear effects, and is not due to R_λ. Further, the influence of these parameters on the exponents is significantly stronger than that of R_λ.

V. CONCLUSION

In this paper, we have examined the effects of the large-scale intermittency and the mean shear rate on various scaling range exponents in the far field of an axisymmetric jet $(x/d=40)$. Specifically, we have considered exponents associated with second-order structure functions, autocorrelations of dissipation rates and power spectra of both the longitudinal velocity fluctuation and the passive temperature fluctuation. All exponents are to varying degrees influenced by the intermittency and the mean shear rate. However, the scalar fluctuation exponents are much more sensitive to these parameters than the longitudinal velocity fluctuation exponents. It is also noted that the influence of these two parameters is significantly greater than that of the Reynolds number R_λ. The scope of the present study was somewhat limited by the

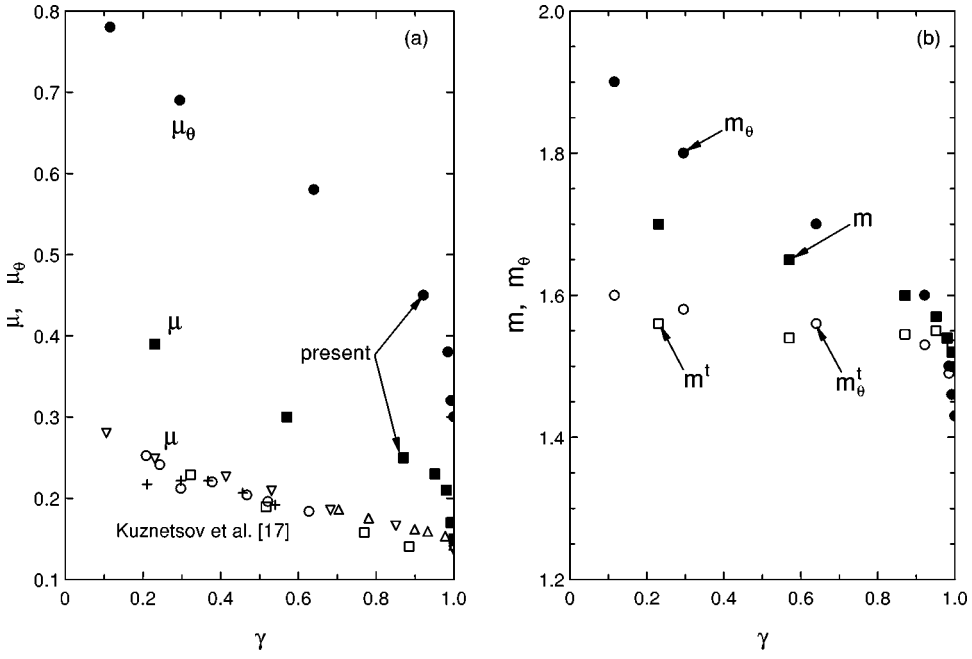

FIG. 9. Effect of the intermittency factor γ on the scaling-range exponents of dissipation rate autocorrelations (μ, μ_θ) and frequency spectra (m, m_θ) of u and θ: (a) μ and μ_θ; and (b) m and m_θ.

fact that only u was measured. It would be useful, in the future, to measure all three velocity fluctuations as well as θ. This would allow the exponents of the spectrum associated with the turbulent energy $\langle q^2 \rangle$ ($\equiv \langle u^2 \rangle + \langle v^2 \rangle + \langle w^2 \rangle$) to be compared with the temperature spectrum exponent. This comparison is likely to be more meaningful [32–34] than one where only the characteristics of u are compared with those of θ.

ACKNOWLEDGMENT

J.M. and R.A.A. gratefully acknowledge the support of the Australian Research Council.

[1] A. N. Kolmogorov, Dokl. Akad. Nauk SSSR **30**, 299 (1941).
[2] K. R. Sreenivasan and B. Dhruva, Prog. Theor. Phys. Suppl. **130**, 103 (1998).
[3] A. N. Kolmogorov, J. Fluid Mech. **13**, 82 (1962).
[4] A. M. Obukhov, J. Fluid Mech. **13**, 77 (1962).
[5] A. S. Monin and A. M. Yaglom, *Statistical Fluid Mechanics* (MIT Press, Cambridge, MA, 1975), Vol. II, Chap. 8.
[6] S. Corrsin, J. Appl. Phys. **22**, 469 (1951).
[7] H. L. Grant, R. W. Stewart, and A. Moilliet, J. Fluid Mech. **13**, 237 (1962).
[8] H. L. Grant, B. A. Hughes, W. M. Vogel, and A. Moilliet, J. Fluid Mech. **34**, 423 (1968).
[9] H. A. Becker, H. C. Hottel, and G. C. Williams, J. Fluid Mech. **30**, 285 (1967).
[10] F. H. Champagne, J. Fluid Mech. **86**, 67 (1978).
[11] J. P. Clay, Ph.D. thesis, University of California San Diego, 1973.
[12] K. R. Sreenivasan, Proc. R. Soc. London, Ser. A **434**, 165 (1991).
[13] K. R. Sreenivasan, Phys. Fluids **8**, 189 (1996).
[14] L. Mydlarski and Z. Warhaft, J. Fluid Mech. **320**, 137 (1996).
[15] L. Mydlarski and Z. Warhaft, J. Fluid Mech. **358**, 135 (1998).
[16] R. A. Antonia, and R. J. Smalley, Phys. Rev. E **63**, 025301 (2001).
[17] V. R. Kuznetsov, A. A. Praskovsky, and V. A. Sabelnikov, J. Fluid Mech. **243**, 595 (1992).
[18] D. R. Dowling and P. E. Dimotakis, J. Fluid Mech. **218**, 109 (1990).
[19] J. Mi, in Proceedings of the 8th Asian Congress of Fluid Mechanics, Shenzhen 1999, edited by E. Cui (unpublished), p. 137.
[20] J. Mi, D. Nobes, and G. J. Nathan, J. Fluid Mech. **432**, 91 (2001).
[21] J. Mi and R. A. Antonia, Exp. Therm. Fluid Sci. **8**, 328 (1994).
[22] J. Mi and R. A. Antonia, Phys. Fluids **6**, 1548 (1994).
[23] R. W. Bilger, R. A. Antonia, and K. R. Sreenivasan, Phys. Fluids **19**, 1471 (1976).
[24] I. Wygnanski and H. Fiedler, J. Fluid Mech. **38**, 577 (1969).
[25] R. A. Antonia and J. Mi, J. Fluid Mech. **250**, 531 (1993).
[26] M. Namazian, R. W. Schefer, and J. Kelly, Combust. Flame **74**, 147 (1988).
[27] R. A. Antonia, E. J. Hopfinger, Y. Gagne, and F. Anselmet, Phys. Rev. A **30**, 2704 (1984).
[28] F. Anselmet, Y. Gagne, E. J. Hopfinger, and R. A. Antonia, J. Fluid Mech. **140**, 63 (1984).
[29] K. R. Sreenivasan and R. A. Antonia, Annu. Rev. Fluid Mech. **29**, 435 (1997).
[30] T. Y. Hou, X.-H. Wu, S. Chen, and Y. Zhou, Phys. Rev. E **58**, 5841 (1998).
[31] B. R. Pearson, Ph.D. thesis, University of Newcastle, 1999.
[32] R. A. Antonia, Y. Zhu, F. Anselmet, and M. Ould-Rouis, Phys. Fluids **8**, 3105 (1996).
[33] R. A. Antonia, M. Ould-Rouis, F. Anselmet and Y. Zhu, J. Fluid Mech. **332**, 395 (1997).
[34] R. A. Antonia and R. J. Smalley, Phys. Rev. E **62**, 640 (2000).